Engineering Transactions, **73**(2): 177–197, 2025, https://doi.org/10.24423/engtrans.3440.2025
Institute of Fundamental Technological Research Polish Academy of Sciences (IPPT PAN)
Université de Lorraine • Poznan University of Technology

Research Paper

Investigation of a Vibratory Stress Relief System for Hard-Turned EN 31 Components

Pankaj BHOKARE*, Vishal VASISTHA

Department of Mechanical Engineering, Monad University
Hapur, Uttar Pradesh, India

*Corresponding Author e-mail: bhokarepankaj79@gmail.com

This study examines the use of artificial neural networks (ANNs) to forecast and optimize residual stress and Brinell hardness in EN 31 components subjected to vibratory stress relief (VSR). The influence of important process parameters – amplitude, frequency, and time – was determined through comprehensive ANOVA analyses. According to the findings, residual stress and Brinell hardness are substantially influenced by amplitude, while frequency plays a crucial role in managing stress and hardness before VSR. The significance of time varied across different processes. The ANN model consistently demonstrated high predictive accuracy, achieving 99.82% for Brinell hardness after VSR, 98.27% for residual stress after VSR, 99.98% for Brinell hardness before VSR, and 98.20% for residual stress before VSR. Model performance was further improved through data transformation and normalization. A robust framework for optimizing VSR process parameters was established by integrating ANOVA and ANN, which enabled precise control over mechanical properties. This research emphasizes the potential of ANN in predictive modeling and process optimization in materials engineering, providing valuable insights for enhancing the performance and reliability of mechanical components through customized VSR processes.

Keywords: vibratory stress relief (VSR); residual stress; Brinell hardness; artificial neural network.

1. Introduction

Machining is an essential material removal procedure that inevitably generates residual stress, a key indicator of the quality and performance of the machined workpiece. Residual stresses directly impact fatigue life, fracture behavior, wear resistance, and corrosion resistance [1]. Residual stresses necessitate post-processing to eliminate tensile residual stresses or components must be manufactured with over-tolerant specifications. Therefore, a rapid and precise method for predicting residual stresses in machined components, taking into

account the material properties and process parameters, is essential [2]. Residual stresses arise due to incompatibility between the surface layer and the bulk material. Consequently, any mechanism that alters the shape or geometry of a surface layer can contribute to residual stress formation. These mechanisms can be classified into three categories: mechanical (plastic deformation), thermal (thermal plastic flow), and physical (specific volume variation). The resulting residual stresses are a superposition of those generated by each mechanism, and multiple mechanisms may be present at the same time [3]. EN 31 is a high-carbon alloy steel known for its high strength, wear resistance, and dimensional stability under operational stresses. Its unique properties make it an ideal choice for high precision components requiring durability, such as bearings, tools, and automotive parts.

Vibration (or vibratory) stress relief (VSR) is a sophisticated stress-relieving technique that applies cyclic loading (vibration) to a workpiece, reducing residual stress within minutes, while consuming minimal energy [4]. The objective of residual stress relief is to decrease excessively high stress levels rather than eliminate them entirely. Residual stress fields in materials can be modified through thermal, mechanical, electrical, or magnetic energy applied for a specific duration. Thermal stress relief (TSR) and VSR are conventional technologies that are widely implemented. Nevertheless, other technologies, such as deep cryogenic treatment, shot peening, explosive treatment, hammer peening, electrical or magnetic treatment, and fortification, are effective only in specific cases [5]. VSR has been proposed as an alternative stress relief method for several years. By vibrating a component at a specific frequency and amplitude for a brief duration, it is possible to minimize energy consumption and pollution. However, its industrial adoption remains limited due to the lack of a comprehensive understanding of its mechanism. Residual stress cannot be reduced if the applied vibration is insufficient. Additionally, it is challenging to determine the extent of residual stress reduction by VSR due to the high cost and time-consuming nature of residual stress measurements. Advancements in modeling technology have enabled the simulation of VSR using commercial finite element software such as Marc [6]. This study pioneers the application of VSR for hard-turned EN 31 components through artificial neural networks (ANNs) for predictive modeling and parameter optimization. This approach addresses the critical gap in understanding and implementing VSR for high-carbon alloy steel components while offering environmental and economic advantages over traditional methods.

2. Literature review

Research on VSR primarily concentrates on two aspects: the selection of vibration parameters, such as exciting force, frequency, and vibrating dura-

tion [7, 8], and its impact on stress relief, fatigue life, and dimensional stability [9, 10]. Gong *et al.* [11] reported that frequency is the dominant factor in reducing transverse and longitudinal residual stresses, with optimal results observed at 1000 Hz for SiCp/6061Al composites. In contrast, Wang *et al.* [12] showed that amplitude is more important in residual stress reduction for AZ31 Mg alloys, especially in stress concentration zones. He *et al.* [13] further noted that at lower amplitudes, frequency effects were less pronounced, whereas higher vibration amplitudes were required to induce sufficient plastic deformation for effective stress relief in quenched Cr12MoV specimens. Meanwhile, Shalvandi *et al.* [14] showed that simultaneous tuning of both amplitude and frequency is necessary for ultrasonic vibratory stress relief (UVSR) of stainless steel specimens, highlighting the complex interaction between these parameters.

An arithmetical model for residual stress was developed by Sharma and Pandey [15] through experiments based on response surface methodology (RSM). Their ANOVA results revealed that residual stress generation is substantially influenced by feed rate. Additionally, they elucidated the thermo-mechanical mechanisms responsible for residual stress by highlighting key relationships among machining conditions. Vardanjani *et al.* [16] conducted an experiment to mitigate residual stress. The eccentric cam-like element of the chuck connected the beam to the spindle, while the tool receptacle clamped it. The rotating spindle compelled the cam to generate cyclic loading, which was applied to the beam. Xueping *et al.* [17] optimized process parameters for residual stress through experimental studies. The Taguchi orthogonal array (L9), considering feed rate, cutting speed, and depth of cut (DOC) as rotating parameters, was employed for their investigation. Feed rate, cutting speed, and DOC are the rotating parameters employed. Residual stresses were measured using the X-ray diffraction method. VSR treatment is frequently employed in welding, foundry, and other industries due to its exceptional effectiveness and cost efficiency. However, research on hard-turned EN 31 machined components and aluminum parts remains limited, highlighting the need for further studies.

Stress fluctuations in stainless weldments was investigated by Rao *et al.* [18] using a fatigue testing instrument. Their study highlights the importance of addressing critical aspects of VSR theory. According to the standard model proposed by Klotzbucher and Kraft [19], stress is alleviated when the combined effect of residual stress and vibratory stress exceeds the material's yield strength. Once the vibrational amplitude decreases, it is assumed that subsequent plastic flow allows the previously stressed area to revert to a lower residual stress level. This is because the plastic deformation processes of metals are indicative of dislocation movement. Dislocation segments are believed to migrate toward a more stable configuration when released from weakly pinning point defects as a result of internal pressures and thermally generated lattice

vibrations. Walker *et al.* [20] observed that dislocation mushrooming occurred as the vibration increased and terminated at the end of the vibration cycle. This suggests that strain decreased as dislocation density increased. These observations indicate that strain energy is released during vibration as a consequence of dislocation proliferation.

Gao *et al.* [10], Sun *et al.* [21], and Yang [22] conducted research on VSR technology, which employs electric motors with eccentric masses to induce vibrations in treated parts at frequencies close to their resonance frequencies. This method has been found to be more reliable than thermal aging in reducing residual stress. VSR is an environmentally friendly, high-efficiency, and low-cost technology; however, it is ineffective for components when the excitation frequency is lower than their inherent frequency. In such cases, the injected vibratory stress distribution becomes irregular due to the low excitation frequency and extended wavelength, which leads to uneven release of residual stress throughout the region. Stress relief in Al-Mg-Si-Cu alloys was examined by Wang *et al.* [23]. In addition, they measured residual stress using X-ray diffraction (XRD). They arrived at the conclusion that the microstructure is influenced by cyclic force. Du *et al.* [24, 25] investigated tension reduction in the photoresist SU-8 layer, attributing internal tension reduction to vibrational effects on cross-linked networks, such as defect removal, increased homogeneity, and local damage repair. Their study indicates that UVSR technology can be applied to nonmetallic objects.

UVSR was investigated in rectangular cross-section slender rods by Zhang and Wang [26] and Wang *et al.* [27]. Their experimental results demonstrated significant residual stress alleviation, identifying initial and extra-vibratory stresses as critical conditions for effective UVSR. Although a few UVSR applications have been presented in recent years, most studies have focused on Almen samples or thin rods, with only a few addressing welded structures and machined components Additionally, the majority of the existing research consists of feasibility studies lacking a comprehensive examination of the UVSR's characteristics and operating mechanisms. VSR technology has been extensively utilized for residual stress relief in welded structures; however, there is still a scarcity of literature on its application to small machined components. A computational model was employed to further examine the concept of VSR treatment [28]. The frequency and amplitude of vibration are the primary parameters in VSR. Both resonant and non-resonant vibrations can conditionally reduce the magnitude of residual stresses, but resonant vibrations are the most effective in the treatment of VSR.

This study examines the utilization of sub-resonant vibrations as a cost-effective and feasible alternative for VSR. We employed sub-resonant VSR to mitigate residual tension due to the machine component's exceptionally high

natural frequency. The objective of this investigation is to improve the stability of hard-turned EN 31 components by dispersing induced residual stresses and reducing workpiece deformation. This concept forms the basis for experimental validation. A method to enhance the stability of hard turned EN 31 machine components is devised by examining the impact of VSR on their dimensional stability. Since the amplitude and frequency have been shown to play a critical role in residual stress relief across various materials, this study takes a systematic approach to evaluate the effect of these parameters on EN 31, a material for which VSR-specific research is limited. To achieve this, this research integrates ANN and the Taguchi method within existing predictive and optimization frameworks, tailoring them to this new context.

3. Methodology

3.1. Experimental test setup

EN 31, a high-carbon alloy steel is used in applications that require high wear resistance and dimensional stability. The chemical composition of EN 31 is approximately 1.0% carbon, 1.5% chromium, 0.3% manganese, and trace amounts of silicon and sulfur. Its mechanical properties include a tensile strength of 750 MPa and a Rockwell hardness of 55 HRC. Due to the high residual stress levels after machining, EN 31 is an ideal candidate for testing the effectiveness of VSR and its efficient stress relief processes. This study examines the efficacy of a VSR system on hard-turned EN 31 components. Vibration frequency, vibration amplitude, and treatment time were the input parameters chosen for this investigation. Specifically, vibration frequency (F) levels were established at 750, 850, 950, and 1050 Hz. Treatment time (T) was also established at 3, 5, 6, and 7 minutes, while the vibration amplitude (A) was varied at 3, 5, 6, and 7 mm.

To cover a frequency range that is within both sub-resonant and near-resonant conditions, the vibration frequency range of 750–1050 Hz was selected, which is also consistent with the natural frequencies of EN 31 components as suggested by Gong *et al.* [11]. Following He *et al.* [13], amplitudes levels between 3–7 mm were selected, as they have been shown to induce plastic deformation in hardened steels without causing surface damage. Additionally, based on the findings of Wang *et al.* [12], treatment times between 3–7 minutes were selected, as times shorter than 3 minutes did not provide significant stress relief, while times greater than 7 minutes showed diminishing returns.

The selected parameters and their respective levels were based on empirical data and previous research to capture the essential interactions influencing the residual stress relief process. Residual stress and Brinell hardness were the

primary output parameters that were measured. An X-ray diffraction technique was employed to measure residual stress both before and after the VSR process. The residual stress was measured with an XRD system with Cu Kα radiation as a source. A step size of 0.02° was used to analyze the diffraction angles within the range of $2\theta = 30° - 130°$. Stress variations were quantified by calculating stress values using peak broadening and the $\sin^2\psi$ method, ensuring accurate measurement of residual stress before and after VSR. The machined surfaces were prepared for Brinell hardness testing by using sandpapers of different grit sizes (240–1200) to obtain a mirror finish. This preparation also helped ensure uniformity and accuracy in hardness measurements. Before and after the VSR treatment, Brinell hardness was then evaluated using a Brinell hardness tester, applying a load of 2942 N with a 10 mm steel ball. A digital optical microscope was used to measure the indentation diameter for precise hardness calculation. The mechanical and surface properties of the EN 31 components were examined in order to gain a thorough understanding of the effects of the VSR process. Consequently, these output parameters were chosen.

Several constant parameters and assumptions were maintained to ensure the consistency and reliability of the experimental results. In order to guarantee uniform material properties, all EN 31 components were obtained from the same batch. The experiments were conducted in a controlled environment at a constant temperature of 25°C and a humidity level of 50%. To prevent variations caused by equipment differences, all components were machined using the same turning machine and parameters. Figure 1 illustrates the experimental VSR configuration utilized in this investigation. The studied workpiece is a bar of EN 31, hardened to 55 Rockwell hardness. The test sections were machined on a CNC turning center to minimize discrepancies in the conducted trials. The turned test pieces are illustrated in Fig. 2, while the actual VSR setup is de-

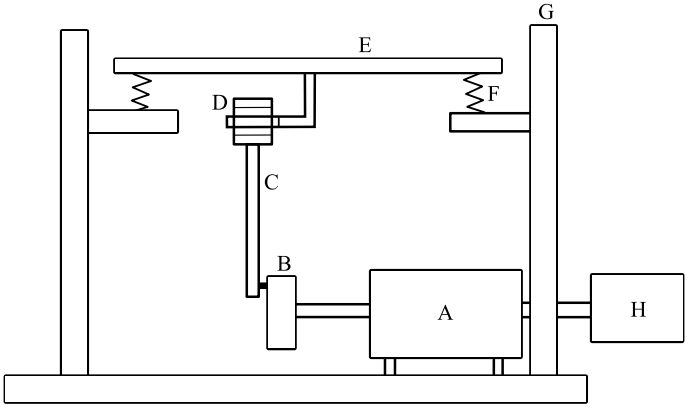

FIG. 1. Schematic of the VSR test setup: A – motor, B – eccentric disc, C – connecting rod, D – bearing, E – exciter table, F – spring G – support, H – DC supply.

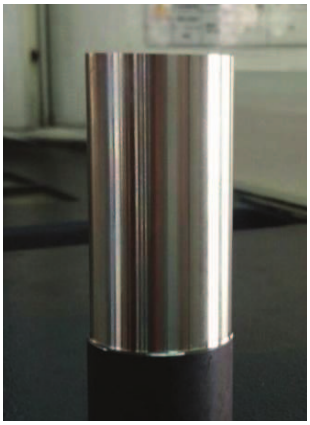

FIG. 2. Turned test piece.

picted in Fig. 3. The experimental apparatus consisted of a frequency controller, an eccentric disc connected to an electric motor, and a mechanically actuated vibration shaker that was used for adjusting the vibration amplitude.

FIG. 3. Photograph of the acual test setup used for VSR.

3.2. Taguchi DOE

The effects of the specified input parameters on the output responses were systematically investigated using the Taguchi design of experiments (DOE) approach. To minimize the number of experimental trials while maintaining the essential interactions between factors, an L16 orthogonal array was implemented. Taguchi DOE is a design methodology that is both robust and effective for opti-

mizing process parameters, which enhances both performance and quality. The interaction between multiple factors at various levels can be studied in a structured and efficient manner by using the orthogonal array. Table 1 lists the levels and factors selected for the Taguchi experimentation, where four levels and three factors were chosen.

Table 1. Factor information and levels.

Symbol	Factors	Level 1	Level 2	Level 3	Level 4
X1	Amplitude [mm]	3	5	6	7
X2	Frequency [Hz]	750	850	950	1050
X3	Time [s]	3	5	6	7

For the selected factors and levels, a Taguchi L16 orthogonal array was selected, and the corresponding results for residual stress before and after VSR are provided in Table 2.

Table 2. Taguchi orthogonal array and results.

Amplitude [mm]	Frequency [Hz]	Time [s]	Residual stress after VSR [N/mm^2]	Residual stress before VSR [N/mm^2]
3	750	3	60.3	67.0
3	850	4	7.5	8.5
3	950	5	89.0	99.0
3	1050	6	156.5	174.3
5	750	4	13.9	15.3
5	850	3	252.8	280.9
5	950	6	194.5	216.0
5	1050	5	267.4	297.1
6	750	5	237.5	263.9
6	850	6	287.4	319.3
6	950	3	544.0	604.5
6	1050	4	493.6	548.5
7	750	6	192.0	213.2
7	850	5	62.0	68.7
7	950	4	66.5	74.0
7	1050	3	485.0	539.0

3.3. Data analysis

A systematic approach was employed to evaluate the effectiveness of the VSR system on EN 31 components during the data analysis for this research. The

focus was on residual stress and Brinell hardness, both before and after the VSR process. Data were initially acquired for each experimental run, including residual stress and Brinell hardness measurements, across varying levels of the input parameters: vibration frequency (F), vibration amplitude (A), and treatment time (T). The data that was collected were subsequently subjected to regression analysis using an ANN model. Additionally, the input parameters were used to predict the values of residual stress and Brinell hardness using the ANN model. The model's accuracy was evaluated by comparing the predicted values to the actual experimental values. Subsequently, the absolute percentage error and the percentage error between the actual and predicted values were computed for each experimental run to identify the deviation between the two.

The data were standardized to ensure a fair comparison across various experimental trials. In order to guarantee that all variables were comparable and to facilitate an accurate evaluation of the VSR process's efficacy, the residual stress and Brinell hardness values were normalized to a common scale. Afterward, the experimental trials were ranked using the technique for order of preference by similarity to ideal solution (TOPSIS) method, a multi-criteria decision-making approach. The proximity of each run to the ideal solution was assessed by TOPSIS. The optimal combination of input parameters for the VSR procedure was determined by analyzing the standardized data using TOPSIS. Ultimately, the rankings from the TOPSIS analysis were compared with the predicted values derived from the ANN model, with the results being verified through confirmatory experiments. The optimal conditions for the VSR process were confirmed by these experiments, ensuring the consistency and reliability of the findings. The VSR system's impact on the mechanical properties of EN 31 components was comprehensively assessed through this structured data analysis. This approach guaranteed precise predictions, dependable outcomes, and a comprehensive evaluation of the most effective process parameters.

4. Results and discussion

4.1. ANN predictions

In this study, the residual stress and Brinell hardness of EN 31 components were predicted both before and after the VSR procedure using an ANN model. The hyperparameters of the ANN were optimized to enhance its performance, and the selected values are shown in Table 3.

Substantial insights into the prediction of residual stress and Brinell hardness in EN 31 components subjected to VSR were obtained through the implementation of the ANN in this research. The ANN model enabled a deeper understanding of the VSR process and its optimization by accurately predicting these

Table 3. ANN hyperparameters tuning.

Parameter	Value
Number of layers	2
Units (neurons)	9
Epochs	400
Batch size	5
Verbose	0
Kernal initializer	Normal
Activation (layer 1)	ReLu

mechanical properties. The ANN model was trained and tested on data from various combinations of amplitude, frequency, and treatment duration. The following section presents the comprehensive results and discussions derived from the model's predictions.

The ANN model demonstrated a high predictive accuracy of 99.82% for Brinell hardness after VSR. The model's ability to capture the complex relationships between the input parameters and the resulting hardness was demonstrated by the fact that the predicted values closely matched the actual experimental results. The ANN model's capability to accurately represent the nonlinearities and interactions between amplitude, frequency, and time, which are critical factors influencing the post-VSR hardness of EN 31 components, is indicated by the minimal deviations between the actual and predicted values. Table 4 provides a comparison of the actual Brinell hardness values after VSR and the predicted values.

Table 4. Brinell hardness after VSR (ABH) and predicted ABH values.

A	F	T	Actual Brinell hardness (ABH)	Predicted ABH
6	1050	5	1.121358	1.123991013
7	750	7	1.121336	1.118565202
7	850	6	1.121321	1.121639729
7	950	5	1.121299	1.123194933
7	1050	3	1.121285	1.123978615

The ANN model also demonstrated strong predictive capacity for residual stress following VSR, with an accuracy of 98.27%. The model's ability to understand the intricate factors that influence residual stress reduction through VSR is emphasized by its high level of accuracy. Table 5 provides a comparison of the actual residual stress (ARS) values after VSR and the predicted ones. The model's predictions were consistent with the experimental data, indicating its capacity to accurately reflect the influence of the VSR parameters on residual

Table 5. Residual stress after VSR (ARS).

A	F	T	ARS	Predicted ARS
6	1050	5	1.123387	1.110567331
7	750	7	1.122605	1.100653291
7	850	6	1.127225	1.10589242
7	950	5	1.128862	1.108870506
7	1050	3	1.131787	1.110574245

stress outcomes. The ANN model achieved an exceptional accuracy of 99.98% in predicting Brinell hardness prior to VSR. This suggests that the model is capable of accurately simulating the hardness characteristics of EN 31 components before they are subjected to VSR treatment. Table 6 provides a comparison of the actual Brinell hardness values prior to VSR and the predicted values. The ANN model's ability to accurately capture the pre-VSR hardness characteristics, which are crucial for optimizing initial process parameters, is demonstrated by the close alignment between actual and predicted values.

Table 6. Brinell hardness before VSR (BBH).

A	F	T	BBH	Predicted BBH
6	1050	5	1.122031	1.121869087
7	750	7	1.122052	1.121688008
7	850	6	1.122066	1.121811271
7	950	5	1.122073	1.121854067
7	1050	3	1.122087	1.121869087

The model's exceptional performance in mapping the initial stress states of the material is evidenced by its 98.20% accuracy in predicting residual stress prior to VSR. The model's ability to accurately represent the initial residual stress conditions influenced by the set parameters is further indicated by the minimal discrepancies between the actual and predicted BRS values. Table 7

Table 7. Residual stress before VSR.

A	F	T	BRS	Predicted BRS
6	1050	5	1.125751	1.109902024
7	750	7	1.127902	1.108927608
7	850	6	1.12985	1.109506607
7	950	5	1.132007	1.109775901
7	1050	3	1.134169	1.109901309

provides a comparison of the actual residual stress values prior to VSR and the predicted ones. The robustness and reliability of the ANN model for predictive analysis in the context of VSR processes are demonstrated by its consistently high accuracy across all predicted parameters (ABH, ARS, BBH, and BRS). These findings underscore the critical influence of amplitude, frequency, and time on the Brinell hardness and residual stress of EN 31 components. The ANN model's precise predictions establish a strong foundation for optimizing the VSR process. By understanding the impact of variations in amplitude, frequency, and time on outcomes, the process can be optimized to accomplish the desired material characteristics with greater precision The reliability and efficacy of the ANN model in predictive modeling for mechanical properties are underscored by its successful application in this study. Due to its ability to capture non-linear relationships and interactions, the ANN model proves to be a valuable tool in materials science and engineering research.

After VSR, the ANN model showed a very high accuracy of 99.82% for Brinell hardness and 98.27% for residual stress. The ANN model performs much better than traditional regression models, which typically achieve accuracy rates between 85% and 90% on similar datasets [11]. The ability of the ANN to capture nonlinear interactions and the complex relationships between vibratory parameters and material properties, factors that traditional models often struggle to address, is what made this enhancement possible.

4.2. ANOVA analysis

An analysis of variance (ANOVA) was performed to determine the impact of the input parameters (amplitude – A, frequency – F, and time – T) on the output responses (residual stress before VSR – BRS, residual stress after VSR – ARS, Brinell hardness before VSR – BBH, and Brinell hardness after VSR – ABH). The ANOVA results provide a comprehensive understanding of the factors that significantly impact the responses and help identify the most appropriate levels for these factors. According to the ANOVA analysis for BRS, residual stress before VSR was significantly influenced by the amplitude (A) and frequency (F), with p-values of 0.000 and 0.001, respectively. No significant factor was identified with a p-value of 0.071 for time (T). Table 8 presents the analysis of variance for residual stress before VRS (BRS).

It is shown that treatment time has a limited effect on certain responses, e.g., residual stress, due to the dominance of amplitude and frequency in exciting plastic deformation and stress relaxation mechanisms. When the amplitude-induced energy exceeds the material's yield threshold, the role of time becomes secondary to the amplitude-induced energy. As Wang *et al.* [12] suggested, the duration of vibration is overridden by the amplitude-induced energy. In addition,

TABLE 8. Analysis of variance for residual stress before VSR (BRS).

Source	DF	Adj. SS	Adj. MS	F-value	p-value
A	3	0.002560	0.000853	265.66	0.000
F	3	0.000230	0.000077	23.83	0.001
T	3	0.000038	0.000013	3.97	0.071
Error	6	0.000019	0.000003	–	–
Total	15	0.002847	–	–	–

the inherent high hardness in EN 31 components mitigates the effects of long-term vibrations on stress redistribution.

The residual stress prior to VSR is depicted in Fig. 4, which demonstrates the impact of amplitude, frequency, and time. The plot emphasizes the substantial influence of frequency and amplitude on BRS, with amplitude having the most

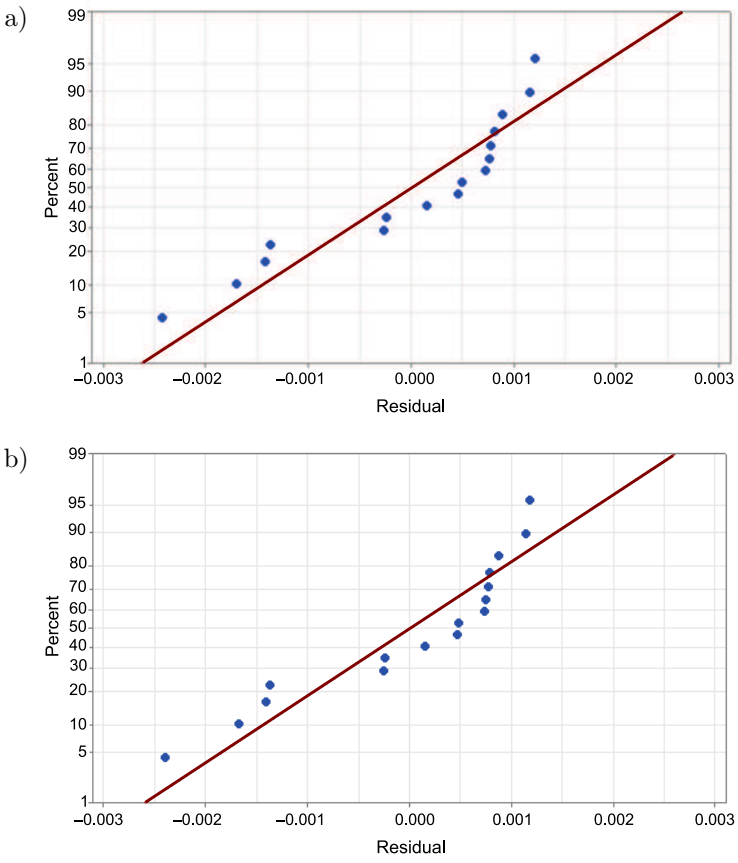

FIG. 4. Normal probability plots of residual stress:
a) before VSR, b) after VSR.

significant impact. This implies that the residual stress prior to the treatment can be substantially diminished by adjusting the amplitude during the VSR procedure. The frequency also plays a critical role, suggesting that tension levels can be influenced by higher or lower frequencies. Nevertheless, the time parameter exhibits a less significant effect, suggesting that the residual stress prior to treatment is minimally affected by the duration of the VSR process. Equation (4.1) provides the regression equation for the residual stress (BRS) before VSR Its critical role in stress relief is due to its ability to induce sufficient plastic deformation, exceeding the material's yield strength in regions of interest. This observation is consistent with Klotzbucher and Kraft [19], who proposed that amplitude-driven plastic flow allows dislocation motion and strain energy dissipation, leading to effective stress relaxation. Amplitude is found to be the consistently significant factor across ANOVA analyses, and its paramount importance in optimizing VSR processes for EN 31 components is emphasized. Figure 4 shows the comparison of normal probability plot for before and after residual stress.

$$\begin{aligned}(4.1)\quad \mathrm{BRS} = {} & 1.11552 - 0.018063A\_3 - 0.004666A\_5 + 0.007270A\_6 \\ & + 0.015459A\_7 - 0.005213F\_750 - 0.001572F\_850 + 0.001857F\_950 \\ & + 0.004929F\_1050 - 0.002202T\_3 - 0.000594T\_5 \\ & + 0.001868T\_6 + 0.000928T\_7.\end{aligned}$$

The p-values of 0.000 indicated that both amplitude (A) and frequency (F) were significant factors in the ANOVA analysis for ARS. The p-value for time (T) was 0.070, which suggests borderline significance. Figure 5 illustrates the influence of amplitude, frequency, and time on Brinell hardness before and after VSR. The plot confirms that amplitude and frequency are substantial contributors to ARS, while time exhibits ambiguous significance. This suggests that the residual stress levels after treatment can be substantially influenced by adjusting the amplitude and frequency during the VSR process. The amplitude's influence is substantial, indicating that precise management of this parameter can yield superior tension relief results. ARS is also affected by the frequency, emphasizing the necessity of carefully selecting vibration frequencies during the VSR procedure. Equation (4.2) presents the regression model for residual stress after VSR (ARS).

$$\begin{aligned}(4.2)\quad \mathrm{ARS} = {} & 1.11222 - -0.017998A\_3 - 0.004648A\_5 + 0.007242A\_6 \\ & + 0.015405A\_7 - 0.007115F\_750 - 0.000844F\_850 + 0.002070F\_950 \\ & + 0.005888F\_1050 - 0.002184T\_3 - 0.000591T\_5 \\ & + 0.001861T\_6 + 0.000914T\_7.\end{aligned}$$

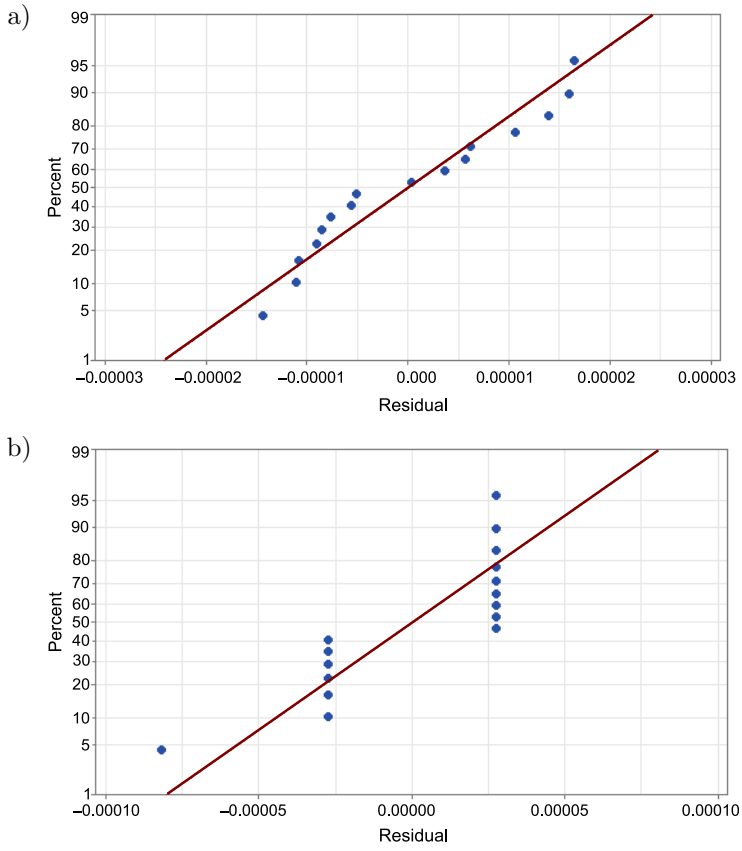

FIG. 5. Normal probability for Brinell hardness before and after VSR
a) BHN before VSR, b) BHN after VSR.

Table 9 presents the analysis of variance for after residual stress (ARS).

TABLE 9. Analysis of variance for after residual stress (ARS).

Source	DF	Adj. SS	Adj. MS	F-Value	p-value
A	3	0.002541	0.000847	270.04	0.000
F	3	0.000361	0.000120	38.38	0.000
T	3	0.000038	0.000013	4.00	0.070
Error	6	0.000019	0.000003	–	–
Total	15	0.002959	–	–	

The ANOVA results for BBH indicated that amplitude (A), frequency (F), and time (T) were all significant factors influencing Brinell hardness prior to VSR, with p-values of 0.000, 0.001, and 0.021, respectively. The substantial

impacts of amplitude, frequency, and time on Brinell hardness prior to VSR are illustrated in Fig. 5. The plot emphasizes the primary impact of amplitude on BBH, with frequency and time also contributing significantly. This implies that the hardness of the material can be substantially altered prior to treatment by adjusting the amplitude. Additionally, frequency is a critical factor, indicating that the hardness can be influenced by varying vibration frequencies. While the time parameter is significant, its impact is less significant than amplitude and frequency. This suggests that the hardness is influenced by the VSR process's duration to a lesser degree. The regression equation for the residual stress before VRS (BRS) is shown in Eq. (4.3). Figure 5 compares the normal probability for Brinell hardness before and after VSR.

$$\begin{aligned}(4.3)\quad \mathrm{BBH} = {} & 1.12188 - 0.000253A\_3 - 0.000051A\_5 + 0.000118A\_6 \\ & + 0.000185A\_7 - 0.000054F\_750 - 0.000016F\_850 + 0.000018F\_950 \\ & + 0.000052F\_1050 - 0.000020T\_3 - 0.000018T\_5 \\ & + 0.000018T\_6 + 0.000020T\_7.\end{aligned}$$

The amplitude (A) was a significant factor in the ANOVA analysis for ABH, with a p-value of 0.015. However, frequency (F) and time (T) were not statistically significant, with p-values of 0.738 and 0.455, respectively. The impact of amplitude, frequency, and time on Brinell hardness following VSR is illustrated in Fig. 4. The diagram emphasizes that amplitude is the most significant factor influencing ABH, while frequency and time have negligible effects. This implies that the post-treatment hardness of the material can be considerably influenced by controlling the amplitude during the VSR process. Consequently, frequency and time appear to have a negligible effect on hardness after treatment, further underscoring the significance of amplitude in the VSR process. Equation (4.4) provides the regression equation for the after-VSR Brinell hardness (ABH).

$$\begin{aligned}(4.4)\quad \mathrm{ABH} = {} & 1.12141 + 0.000072A\_3 + 0.000054A\_5 - 0.000026A\_6 \\ & - 0.000099A\_7 - 0.000015F\_750 + 0.000024F\_850 + 0.000002F\_950 \\ & - 0.000012F\_1050 - 0.000041T\_3 + 0.000014T\_5 \\ & + 0.000014T\_6 + 0.000014T\_7.\end{aligned}$$

It is shown that the material's hardening mechanism is dominated by amplitude-driven plastic deformation, which is why the effects of frequency on post VSR hardness are negligible. In the case of vibration, frequency primarily affects stress relief during the early stages when dislocation motion and stress redistribution occur, as observed by He *et al.* [13]. Nevertheless, the mi-

crostructural changes caused by amplitude, rather than frequency, govern the post-treatment hardness.

Across all response variables (ARS, BBH, ABH, and BRS), amplitude (A) consistently emerged as a significant factor. This implies that the residual stress and Brinell hardness are significantly affected by the adjustment in the amplitude of vibratory stress relief process. Frequency (F) was found to be significant for BRS, ARS, and BBH, but not for ABH. This suggests that while frequency is essential in determining the initial residual stress and hardness, its impact on the post-VSR hardness (ABH) is less pronounced. Time (T) was significant factor for BBH and showed ambiguous significance for ARS. Nevertheless, it did not have a substantial impact on ABH and BRS. This suggests that the duration of the VSR procedure does have some impact. A comparison of the normal probability plots before and after residual stress has been added, with an overlay of the data points. Additionally, box plots have been included to provide visual comparison of the variance and mean shifts between the two conditions, offering a clearer picture of stress relief effectiveness. These results have important implications for cost and energy efficiency. Since amplitude is identified as the most critical factor in VSR, effective stress relief can be obtained while minimizing the reliance on high-frequency equipment and operating energy by optimizing amplitude settings. Moreover, shorter treatment times also contribute to further cost savings, as amplitude-driven processes are more efficient. These findings pave the way for the development of sustainable and economically viable applications of VSR in manufacturing environments.

5. Conclusion

The predictive capabilities of ANN in modeling the residual stress and Brinell hardness of EN 31 components, before and after the VSR procedure were investigated in this study. The study involved applying ANN to predict outcomes based on varying process parameters and conducting through detailed ANOVA analyses to identify the key factors influencing these mechanical properties. The following are the primary findings of the investigation:

- Amplitude (A) was consistently identified as a significant factor in all response variables (BRS, ARS, BBH, and ABH). The substantial influence of amplitude on both residual stress and Brinell hardness is evident from the high F-values and low p-values. The mechanical properties of EN 31 components were optimized by adjusting the amplitude during the VSR procedure.
- Frequency (F) was found to be significant for predicting BRS, ARS, and BBH; however, it had a negligible effect on ABH. This underscores the

significance of selecting appropriate vibration frequencies during the VSR process to effectively manage residual stress and hardness prior to the stress relief.

- Time (T) had a significant impact on BBH and had an ambiguous significance on ARS, while its impact on BRS and ABH was less pronounced. This suggests that while the duration of the VSR process affects hardness and residual stress, the extent of this impact varies depending on the specific stage of the process.
- The ANN model exhibited exceptionally high predictive accuracy for all parameters, with accuracy rates of 99.82% for ABH, 98.27% for ARS, 99.98% for BBH, and 98.20% for BRS. The ANN model's reliability and effectiveness in capturing the complex relationships between the input parameters and the mechanical properties are validated by the minimal percentage errors between the actual and predicted values.
- The predictive capabilities of the ANN model and the regression equations derived from the ANOVA analysis offer valuable insights for optimizing the VSR process parameters. The VSR process can be optimized to accomplish the desired material properties with greater precision by understanding the impact of amplitude, frequency, and time on residual stress and hardness.
- Amplitude was identified as the most critical factor in optimizing VSR. This insight not only enables effective stress relief but also offers significant industrial benefits in terms of cost-efficiency and energy savings. By minimizing reliance on high-frequency equipment and reducing processing times, manufacturers can lower operational costs while maintaining high-quality outputs.
- Moreover, the environmental benefits of VSR, as a low-energy and pollution-reducing alternative to traditional thermal stress relief methods, align well with the increasing focus on sustainable manufacturing practices.
- The integration of ANN with VSR offers a robust predictive framework that enables precise control of mechanical properties such as residual stress and Brinell hardness. This advancement enhances the reliability and durability of machined components, particularly in critical applications requiring stringent performance standards.

Future studies could explore the application of VSR on other high strength materials, such as titanium alloys or superalloys, to further validate the conclusion of this study. Furthermore, research could be extended to industrial components with complex geometries, such as turbine blades or automotive components, to assess the adaptability of VSR in industrial settings. Furthermore, predictive capabilities of VSR could be realized by integrating advanced data-driven approaches, such as deep learning models, with process optimization.

This could result in adaptive VSR systems capable of responding in real-time to material responses.

Statement and Declarations

Funding Sources

No funding has been received for this work.

Conflict of interest

The authors declare that there is no conflict of interest.

References

1. Wan M., Ye X.Y., Wen D.Y., Zhang W.H., Modeling of machining-induced residual stresses, *Journal of Materials Science*, **54**(1): 1–35, 2019, https://doi.org/10.1007/s10853-018-2808-0.

2. Ulutan D., Alaca Erdem B., Lazoglu I., Analytical modelling of residual stresses in machining, *Journal of Materials Processing Technology*, **183**(1): 77–87, 2007, https://doi.org/10.1016/J.JMATPROTEC.2006.09.032.

3. Capello E., Residual stresses in turning: Part I: Influence of process parameters, *Journal of Materials Processing Technology*, **160**(2): 221–228, 2005, https://doi.org/10.1016/J.JMATPROTEC.2004.06.012.

4. Dawson R., Moffat D.G., Vibratory stress relief: a fundamental study of its effectiveness, *Journal of Engineering Materials and Technology*, **102**(2): 169–176, 1980, https://doi.org/10.1115/1.3224793.

5. Lv T., Zhang Y., A combined method of thermal and vibratory stress relief, *Journal of Vibroengineering*, **17**(6): 2837–2845, 2015.

6. Zhao X.C., Zhang Y.D., Ma Y.J., Finite element analysis of vibratory stress relief process, *Applied Mechanics and Materials*, **88–89**: 623–627, 2011, https://doi.org/10.4028/www.scientific.net/AMM.88-89.623.

7. Zhou L., Wang B., Wei Z., Liu K., Vibration stress relief on the machining of SiCp/6061Al composites by multi-scale finite element analysis, *International Journal on Interactive Design and Manufacturing (IJIDeM)*, **17**(4): 1771–1787, 2023, https://doi.org/10.1007/s12008-023-01245-4.

8. Song J., Zhang Y., Effect of vibratory stress relief on fatigue life of aluminum alloy 7075-T651, *Advances in Mechanical Engineering*, **8**(6): 1687814016654379, 2016, https://doi.org/10.1177/1687814016654379.

9. Ebrahimi S.M., Farahani M., Akbari D., The influences of the cyclic force magnitude and frequency on the effectiveness of the vibratory stress relief process on a butt welded connection, *International Journal of Advanced Manufacturing Technology*, **102**(5–8): 2147–2158, 2019, https://doi.org/10.1007/s00170-019-03288-y.

10. Gao H., Zhang Y., Wu Q., Song J., Wen K., Fatigue life of 7075-T651 aluminium alloy treated with vibratory stress relief, *International Journal of Fatigue*, **108**: 62–67, 2018, https://doi.org/10.1016/j.ijfatigue.2017.11.011.

11. Gong H., Sun Y., Liu Y., Wu Y., He Y., Sun X., Zhang M., Effect of vibration stress relief on the shape stability of aluminum alloy 7075 thin-walled parts, *Metals*, **9**(1): 27, 2019, https://doi.org/10.3390/met9010027.

12. Wang J.S., Hsieh C.C., Lai H.H., Kuo C.W., Wu P.T-Y., Wu W., The relationships between residual stress relaxation and texture development in AZ31 Mg alloys via the vibratory stress relief technique, *Materials Characterization*, **99**: 248–253, 2015, https://doi.org/10.1016/j.matchar.2014.09.019.

13. He W., Gu B.P., Zheng J.Y., Shen R.J., Research on high-frequency vibratory stress relief of small Cr12MoV quenched specimens, *Applied Mechanics and Materials*, **157–158**: 1157–1161, 2012, https://www.scientific.net/AMM.157-158.1157.

14. Shalvandi M., Hojjat Y., Abdullah A., Asadi H., Influence of ultrasonic stress relief on stainless steel 316 specimens: A comparison with thermal stress relief, *Materials and Design (1980–2015)*, **46**: 713–723, 2013, https://doi.org/10.1016/j.matdes.2012.11.023.

15. Sharma V., Pandey P.M., Optimization of machining and vibration parameters for residual stresses minimization in ultrasonic assisted turning of 4340 hardened steel, *Ultrasonics*, **70**: 172–182, 2016, https://doi.org/10.1016/j.ultras.2016.05.001.

16. Vardanjani M.J., Ghayour M., Homami R.M., Analysis of the vibrational stress relief for reducing the residual stresses caused by machining, *Experimental Techniques*, **40**(2): 705–713, 2016, https://doi.org/10.1007/s40799-016-0071-3.

17. Xueping Z., Erwei G., Liu C.R., Optimization of process parameter of residual stresses for hard turned surfaces, *Journal of Materials Processing Technology*, **209**(9): 4286–4291, 2009, https://doi.org/10.1016/j.jmatprotec.2008.10.011.

18. Rao D.-L., Chen L.-G., Ni C.-Z., Zhu Z.-Q., The mechanism for vibratory stress relief of stainless steel, *Transactions of the China Welding Institute*, **26**(9): 58–60,64, 2005, http://hjxb.hwi.com.cn/hjxb/en/article/id/20050914.

19. Klotzbucher E., Kraft H., Vibratory stress relieving – an alternative to thermal stress relieving?, [in:] Macherauch E., Hauk V. [Eds.], *Residual Stresses in Science and Technology*, Vol. 1, pp. 959–966, DGM Informationsgesellschaft Verlag, 1987.

20. Walker C.A., Waddell A.J., Johnston D.J., Vibratory stress relief – an investigation of the underlying processes, *Proceedings of the Institution of Mechanical Engineers, Part E: Journal of Process Mechanical Engineering*, **209**(1): 51–58, 1995, https://doi.org/10.1243/PIME_PROC_1995_209_228_02.

21. Sun M.C., Sun Y.H., Wang R.K., The vibratory stress relief of a marine shifting of $35^{\#}$ bar steel, *Materials Letters*, **58**(3–4): 299–303, 2004, https://doi.org/10.1016/S0167-577X(03)00473-7.

22. Yang Y.P., Understanding of vibration stress relief with computation modeling, *Journal of Material Engineering and Performance*, **18**(7): 856–862, 2009, https://doi.org/10.1007/s11665-008-9310-9.

23. Wang J.-S., Hsieh C.-C., Lin C.-M., Kuo C.-W., Wu W., Texture evolution and residual stress relaxation in a cold-rolled Al-Mg-Si-Cu alloy using vibratory stress relief technique, *Metallurgical and Materials Transactions A*, **44**(2): 806–818, 2013, https://doi.org/10.1007/s11661-012-1450-8.

24. Du L.Q., Wang Q.J., Zhang X.L., Reduction of internal stress in SU-8 photoresist layer by ultrasonic treatment, *Science China Series E: Technological Sciences*, **53**(11): 3006–3013, 2010, https://doi.org/10.1007/s11431-010-4136-8.

25. Du L.Q., Wang Q.J., Zhang X.L., Application of ultrasonic stress relief in the fabrication of SU-8 micro structure, *Key Engineering Materials*, **483**: 3–8, 2011, https://doi.org/10.4028/www.scientific.net/kem.483.3.

26. Zhang L., Wang S.Y., Feasibility analysis and experiment research of ultrasonic vibratory stress relief, *Machinery Design and Manufacture*, **2013**(7): 140–143, 2013.

27. Wang R.Y., Wang S.Y., Mechanism analysis and experimental research of the ultrasonic vibration ageing, *Journal of Chinese Agricultural Mechanization*, **36**: 59–62, 2015.

28. Wang J.S., Hsieh C.C., Lin C.M., Kuo C.W., Wu W., Texture evolution and residual stress relaxation in a cold rolled Al-Mg-Si-Cu alloy using vibratory stress relief technique, *Metallurgical and Materials Transactions A*, **44**(2): 806–818, 2013, https://doi.org/10.1007/s11661-012-1450-8.

29. Guo J.K., *Study on Micro Yield Mechanism of Aluminium Alloy Thick Plate Subjected to Vibratory Stress Relief and Experimental Study*, Master's Thesis, Central South University, Changsha, China, 2010.

Received September 9, 2024; accepted version January 31, 2025.
Online first April 8, 2025.